

Research Article

Simulation of Drill String Vibration inside Well Bore due to Riser's Oscillation

N. Al-Batati, F.M. Hashim and K.S. Pao

Mechanical Engineering Department, Universiti Teknologi PETRONAS,

Bandar Seri Iskandar, 31750 Tronoh, Perak, Malaysia

Abstract: This study attempts to explain the motion behavior of the marine riser coupled to drill string when the vortex induced vibration is involved. Vibrations have been reported to have a major effect on drilling performance, affecting the Rate of Penetration (ROP), causing severe damage to drilling tools and also reduces the efficiency of the drilling process. There are two major components of drilling tools that are subjected to vibration, namely the marine riser and the drilling string. Analysis of vibration in the marine riser and drill string are two topical areas that have individually received considerable attention by researchers in the past. While these two subjects are interrelated, borne by the fact that the marine riser encapsulates and protects the drill pipe, they have been little attempt to investigate them together as an assembly. Due to the complexities of the models, simplifying assumptions were made in order to undertake the investigation. Using staggered approach, the results were compared with experimental and simulation data from the open literature. It was found that the maximum displacement with negative damping occurs at low frequency and rotation speed. The addition of vortex shedding forces caused the drill string to deform from its vertical axis and thus increased the risk of failure of drill string and riser.

Keywords: Drill string-riser coupling, drill string vibration, marine riser, vortex induced vibration

INTRODUCTION

Drilling in deepwater presents a significant challenge, drill string failures like washout and twist-off can result in expensive non-productive time and loss of equipment. Analysis by Norwegian oil industry showed that drilling related economic losses exceeding 150 million USD in a 10-year period, distributed over 187 (Norwegian Oil Industry Association, 2010). Drill string vibrations are extremely complex because of the random nature of a multitude of factors such as: bit/formation interaction, drill string/wellbore interaction and hydraulics. In many cases, it becomes a main cause of premature failure of drill string components and drilling inefficiency. On the other hand in offshore operation, the presence of hydrodynamic pressure, sea current and tidal wave further complicate the analysis due to fatigue. In most offshore operation, a riser is needed to protect the drill pipe from the external environment and stabilize the drill pipe when the drilling is performed. Despite extensive research in the last four decades, questions remain unanswered because of the complexity in compounded parameters. (Bailey and Finnie, 1960; Aldushaishi, 2012).

The Vortex-Induced Vibration (VIV) cannot be separated in the design of deepwater riser systems, including drilling, production and export risers. The VIV can produce a high level of fatigue damage on the

riser when exposed to severe current environments in a relative short period of time (Whitney *et al.*, 1983). Partially driven by the need for off shore oil and gas production, numerical simulation of drill string vibration has been an active research area in recent years. The objective of the current study is to explain qualitatively the observed phenomenon of the vortex induced vibration effect at long span riser to drill string vibratory mode and dynamic response, when the drill string has already penetrated the wellbore.

METHODOLOGY

Riser's vibration due to vortex: In the range of cross-flow velocities and riser diameters of practical interest, flow past the riser is characterized by the alternate shedding of vortices forming a "Karman vortex street" in the wake of the riser. A non-dimensional parameter that governs the flow regime is the Reynolds number (Re) defined by:

$$Re = \frac{\rho v L}{\mu} \quad (1)$$

where,

ρ = The density of fluid

v = Velocity of fluid

L = Pipe length/diameter of cylinder

Corresponding Author: F.M. Hashim, Mechanical Engineering Department, Universiti Teknologi PETRONAS, Bandar Seri Iskandar, 31750 Tronoh, Perak, Malaysia

This work is licensed under a Creative Commons Attribution 4.0 International License (URL: <http://creativecommons.org/licenses/by/4.0/>).

Table 1: Riser operating condition

Depth (m)	R_c	Pressure operation (Pa)	Velocity (m/s)
1	1,065,644	1762.44	1.86
60	836,473	704434.00	1.46
100	624,490	1106510.00	1.09
500	486,988	5127230.00	0.85

μ = Dynamic viscosity

When vortex induced vibrations occurred, the direction of vibration is primarily perpendicular to the current causing an increase in the drag force on the vibrating structure. A large increase in drag which affects the stresses, angles and displacement of the riser must be considered during the riser analysis procedure.

The vortex itself excited significantly only when the structure is excited near the resonant condition, i.e., the only significant response of a pure mode whose natural frequency is close to the vortex shedding frequency which increase the stresses and deflections (Sengupta, 1978). The excitation frequency f_n is related with Strouhal number by:

$$f_n = \frac{vS}{D} \quad (2)$$

where,

- f_n = Vortex shedding frequency
- S = Strouhal number
- v = Velocity of current
- D = Effective diameter

The flow passed through the cylinder is a three-dimensional phenomenon since the vortex shedding is not fully correlated along the span. A measure of the average length over which the shedding is correlated is the correlation length (L_c), for stationary cylinders $L_c \sim 2.5$ to $5 D$.

In this research, the vortex shedding was analyzed using 2D model in segmented depth from 1 to 500 m on turbulent current model with fluid dynamic viscosity 0.0015 N s/m^2 . The riser is modeled in segmented area according to a certain depth to analyze the drag forces that appear on the wall surface (Table 1).

The most widely turbulent models were standard K- ϵ and K- ϵ RNG model. In standard k- ϵ model, the eddy viscosity is determined from a single turbulence length scale, so the calculated turbulent diffusion which occurs only at the specified scale, whereas in reality all scales of motion will contribute to the turbulent diffusion. The RNG approach, which is a mathematical technique that can be used to derive a turbulence model similar to the k- ϵ , resulted in a modified form of the epsilon equation which attempts to account for the different scales of motion through changes to the production term. The turbulent model has been analyzed and developed using Re-Normalization Group (RNG) methods to re-normalize the Navier-Stokes

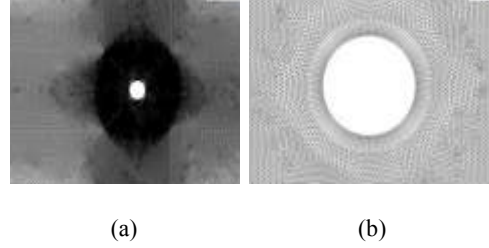


Fig. 1: (a) Domain discretisation used to capture the drag coefficient at the cylinder surface and (b) finer density mesh discretisation around the cylinder

equations, to account for the effects of smaller scales of motion (Dixon and Charlesworth, 2006).

The meshing was split into two regions with the region near the riser having the highest mesh density as shown in Fig. 1. These grids are produced by hyperbolic tangent distribution functions and were used to investigate the effects of the grids on the results of turbulent flow.

Mesh dependency of the numerical solution was conducted to ensure that the solution obtained is convergent and accurate. This is achieved by setting the largest allowable mesh size from 5×10^{-3} to 2×10^{-6} m. Figure 2 showed the vortex velocity around the cylinder for different maximum allowable mesh size. The result showed that with the finer grid at one point the vortex velocity becomes constant and the minimum required grid size is then determined to be 0.125×10^{-5} m.

The computational fluid dynamics simulation will produce an averaged drag coefficient of the cylinder (riser) and this value can be used to calculate the drag force according to Eq. (3). The computed drag force will be used as an input data for the vibration analysis using the Finite Element Method:

$$F_d = \frac{1}{2} C_d v^2 \rho A \quad (3)$$

where,

- F_d = Drag force
- ρ = Fluid density
- C_d = Drag coefficient
- A = Cross section area
- v = Velocity

Drilling string vibration: The three primary modes of vibration are present while drilling, namely axial, torsional and lateral. Field observation recorded these phenomena consist of bit bounce for axial vibration mode, stick/slip for torsion and whirling for lateral vibration mode.

The drill pipe, which is 550 m long encapsulated inside the riser is modeled as 3D Timoshenko's beam elements with six degrees of freedom. This element is based on first order shear deformation theory. The riser,

Table 2: Material properties and parameters used for drill pipe, riser and wellbore

	Drill pipe	Riser	Wellbore concrete
Wall thickness, m	0.0083	0.01	0.01m
Outside diameter, m	0.2032	0.50	0.50m
Young's modulus, GPa	210	210	350
Poisson's ratio	0.3000	0.30	0.30
Density, kg/m ³	7850	7850	2400
Force, kN	100		
Length, m	550	500	50
Rotational velocity, RPM	80 and 300		

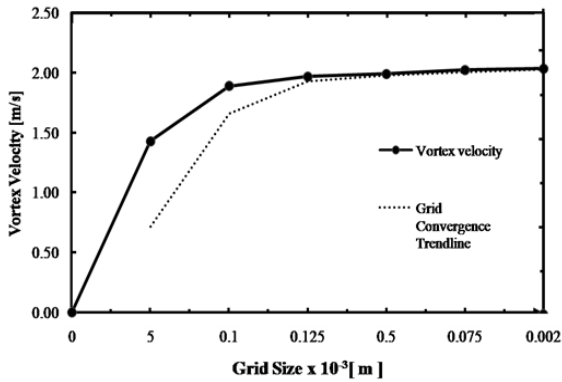


Fig. 2: Vortex velocity convergent versus the maximum allowable mesh size

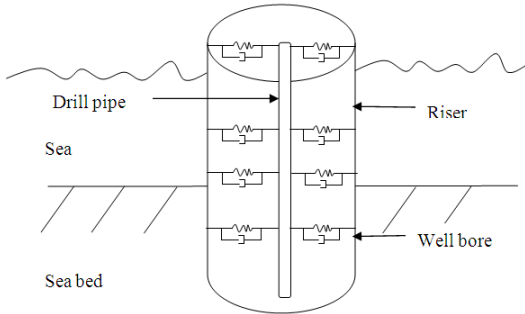


Fig. 3: Schematic of the mechanical model assumption for the drill string riser coupled vibrational analysis

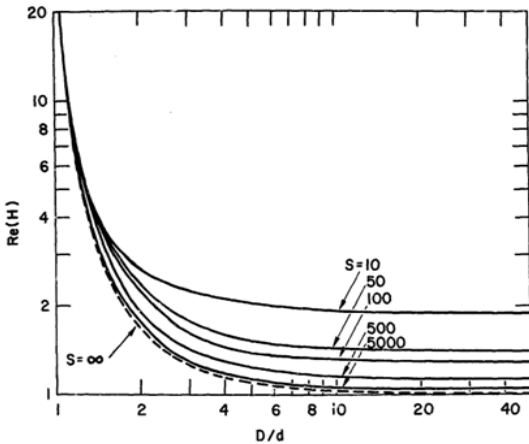


Fig. 4: Real values of H as a function of D/d for selected values of S (Chen *et al.*, 1976)

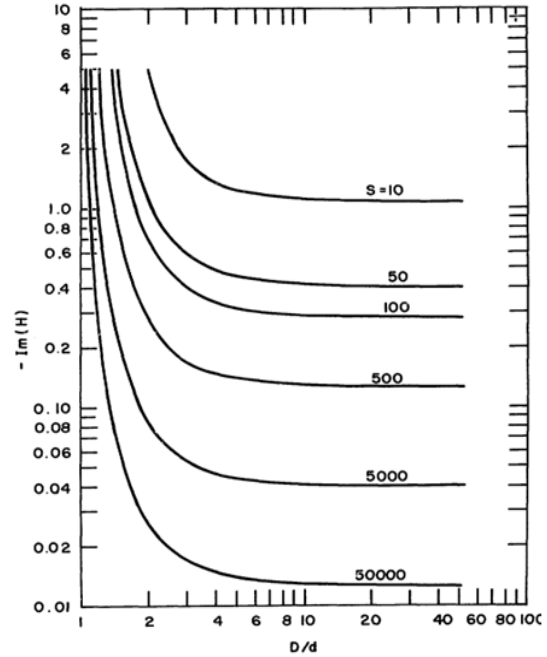


Fig. 5: Imaginary values of H as a function of D/d for selected values of S (Chen *et al.*, 1976)

500 m long, is modeled as 3D shell element and is assumed the same material properties as the drill pipe, which is cast iron. The calculation of drag force and hydrodynamic pressure are inputted as external forces at the external wall of the shell. The 50 m wellbore, which is included in the analysis to mimic the well penetration into subsurface, has its material properties showed in Table 2. It is assumed that the top boundary of the riser and drill pipe are anchored with zero displacement and rotation, respectively. The model of drill pipe and riser are shown in Fig. 3.

Riser-drill pipe coupling: In order for the vibratory forces from the riser to be transmitted to the drill string, an assumption is made such that the returning mud acts as a medium of force transmission thus providing the means for coupling. The mud is modeled as spring-dashpot elements that connect the drill pipe to the riser. Using the displacement method, the spring stiffness and damping coefficient can be obtained as follows. Under the influence of an external force ΔF , the drill pipe will displace by a distant ΔX . According to Bahr Khalil (2009) and Aarsnes Flø (2012), the stiffness now may be defined with:

$$K_{mud} = \frac{\Delta F}{\Delta X} = \frac{AE}{L} \tag{4}$$

where,
 E = The mud variable which is closest to bulk modulus of mud

Table 3: Comparison of drag coefficients

Source	C _D	C _L
Sohankar (2006)	2.31	1.54
Lubcke <i>et al.</i> (2001)	2.26	0.95
Ehsan <i>et al.</i> (2012)	2.13	1.41
Present model	2.19	0.81

Table 4: Comparison on the three main natural frequency of lateral vibration

Source	1 st mode (Hz)	2 nd mode (Hz)	3 rd mode (Hz)
Present work	1.25	2.93	4.18
Zare <i>et al.</i> (2011)	1.23	3.14	4.19
Burgess <i>et al.</i> (1987)	1.25	3.15	NA

A = The virtual spring cross section area

L = Spring length

The effect of mud including added mass and damping can be written, (Chen *et al.*, 1976):

$$\zeta = \frac{1}{2} \left(\frac{M_{mud}}{C_m M_{mud} + M_{pipe}} \right) \text{Im } H \quad (5)$$

M_{mud} is displaced mud mass, Im H is the imaginary value from modified Bessel's function (0.5), C_m is added mass correction factor coefficient (3.7), M_{pipe} is pipe mass. We get $\zeta = 0.01725$. Values of C_m and H are a function of D/d for selected value of S, the non dimensional parameter that describe as:

$$S = \frac{\omega D^2}{\nu} \quad (6)$$

$$C_m = R_e(H) \quad (7)$$

where, ω is the rotational frequency, D is the riser outside diameter and ν is dynamic viscosity of mud. R_e(H) is the real value from modified Bessel's function that related to D/d and S. Figure 4 shows C_m and H will be 3.7 and 0.5, if S and D/d are equal to 475 and 1.32 with outside diameter of drill collar 0.38 m respectively at 190 RPM. It should be noted, because of the low value of 1.32 for diameters ratio, the change in S due to change in ω have little influence on C_m and H values. Hence, assuming the mean speed of ω is used in this calculation (Fig. 5).

VERIFICATION OF VIV AND DRILL STRINGS VIBRATION

Vortex shedding force: Validation for the present model has been performed using previous publication in the open literature (Lien *et al.*, 1997; Sohankar, 2006; Lubcke *et al.*, 2001; Ehsan *et al.*, 2012). The results verified the methodology by recreating the previous turbulence model and analyze it using present

methodology. Table 3 and 4 compared the results of drag and lift coefficients and show a good level of agreement.

Lateral vibration: Zare *et al.* (2011) simulates drill strings lateral vibration inside the well bore. Using Burgess *et al.* (1987) experimental model setup, they modeled both drill string and well bore using shell 3D element and applied 80, 191 and 254 RPM rotational speed. The present research approaches the same model setup using beam element for the drill string and shell element for the well bore. A modal analysis is conducted on the proposed model to obtain the natural frequencies of lateral vibrations. Simulation results compared favorably well with experimental data with percentage error of below 10% recorded, confirming the validity of the current model setup.

RESULTS AND DISCUSSION

Riser vortex force: The simulation of turbulence model using RNG k- ϵ was conducted to attain the maximum drag forces at the riser. To save the iteration memory and simplify the model, the 500 m riser was analyzed only in segmented depth. The drag coefficient of each segmented riser will be transformed to drag force using Eq. (3) and interpolated along the riser's longitudinal direction as external force for the finite element analysis.

Figure 6 shows the drag forces increases in a short time and then remain constant. According to Eq. (3) since the vortex shedding frequency is proportional to the current velocity and the load of intensity of riser is square of the current velocity, the magnitude of the drag force will be approximately constant (Sengupta, 1978).

Table 5 shows the drag forces gradually increase as the riser going deeper. The intensity of hydrodynamic force and the increasing level of salinity contribute to the drag force rising. Figure 7 shows the wake-field velocity contour of riser at 60 m depth. The velocity result shows a significant decrease of velocity from the upstream to the downstream side at the wake-field horizontal axis. A narrow wake with high speed zone also recorded outside the wake field at the top region of cylinder.

Lateral vibration: The lateral vibration is analyzed by inputting the boundary condition and the drag forces output from fluid dynamic to riser's wall. First, modal analysis is performed to determine the vibration characteristics of the structure. The goal of this modal analysis is to determine the mode shapes and the natural frequencies. The analysis used frequency range from 0 to 1000 Hz and the first three natural frequencies are shown in Table 6.

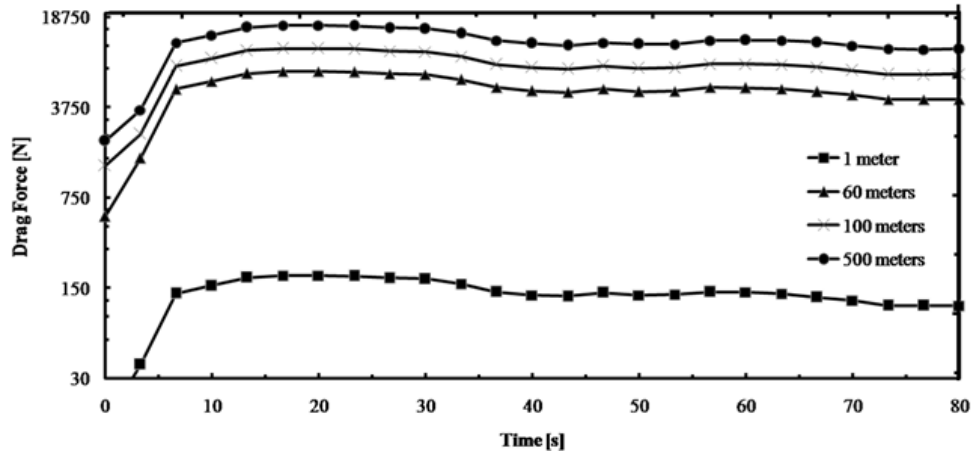


Fig. 6: Calculated riser drag force versus time

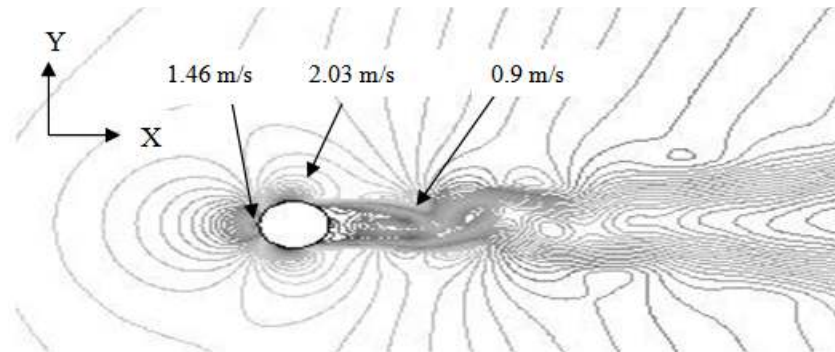


Fig. 7: Riser wake field velocity contour at 60 m depth

Table 5: Drag force summarize

Depth (m)	Force (N)
1	109
60	4310
100	6827
500	7071

Table 6: First three natural frequency result of lateral vibration

Frequency mode	Natural frequency (Hz)
1 st	0.74
2 nd	1.70
3 rd	2.43

Second, the harmonic response analysis solves the equation of motion (12) for linear structures undergoing steady-state vibrations. Any sustained cyclic load will produce a sustained cyclic response of a structure which is often called a harmonic response:

$$M\ddot{u} + C\dot{u} + Ku = f(t) \quad (8)$$

In the above equation M, C, K denotes the structural mass, damping and, stiffness matrices, respectively. \ddot{u} is the vector of nodal accelerations, \dot{u} is the velocity, u is the displacement and f (t) is the vector

of applied force. Harmonic analysis was performed to obtain the displacement and the harmonic response of the system with frequency range from 0 to 50 Hz. A rotation speed of 80 and 300 RPM were applied to the drill string to compensate low and medium speed at the drill pipe.

Vortex shedding force has a big role in changing the shape of drill string displacement. Present analysis observes the relation between drill pipe displacement and vortex forces. Without the presence of vortex forces, the drill strings free oscillation recorded at the longitudinal axis is shown in Fig. 8. The present analysis is similar to the numerical analysis performed by Gulyayev and Borshch (2011), which is presented in Fig. 9 shows the drill string displacement on free modes of vibration in different frequencies.

By the time when vortex shedding forces are included in the system and increase to near resonance, the drill string will deform from its original state and moving repeatedly back and forward from its longitudinal axis and continue with the same mode even the frequency is already above resonance. Figure 10 shows the profile throughout the frequency from 0.5 to 10 Hz.

Table 7: Maximum displacement for riser and drill string

Rotation (RPM)	Drill string displacement inside riser (cm)		Riser displacement (cm)		Drill string displacement inside well bore (cm)	
	0.5 Hz	5 Hz	0.5 Hz	5 Hz	0.5 Hz	5 Hz
80	5.530	2.365	5.378	2.731	1.692	0.897
300	0.247	0.136	1.261	1.651	0.312	0.003

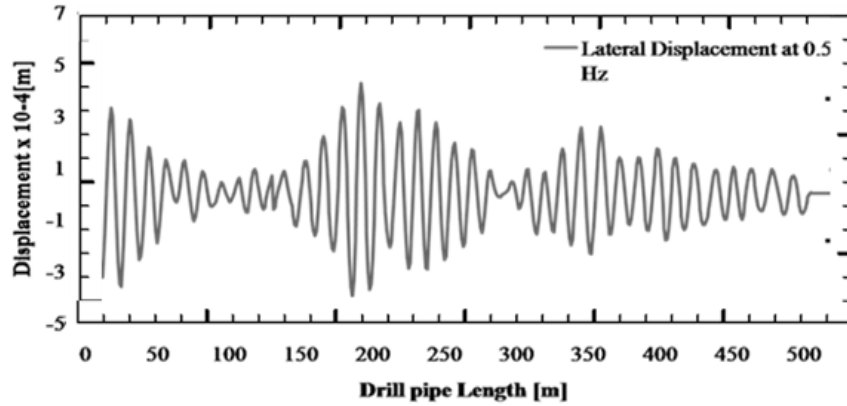


Fig. 8: Lateral displacement mode at 80 RPM without vortex shedding forces

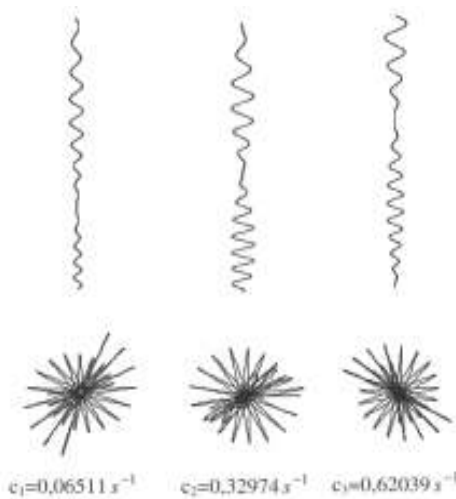


Fig. 9: Modes of free vibration for 500 m drill strings in different frequencies (Gulyayev and Borshch, 2011)

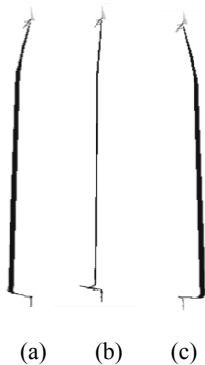


Fig. 10: Lateral displacement plot at different mode of frequency; (a) 0.5 Hz, (b) 5 Hz, (c) 10 Hz

Table 7 shows the maximum displacement at 80 and 300 RPM. Using Strouhal number Eq. (2), the vortex shedding will resonant at 0.5 Hz and shows a rising trend of drill string displacement at 80 RPM. Increasing the frequency to 5 Hz with rotation speed of 300 RPM causes a decrease in the drill string displacement. This is because the VIV vibration was no longer able to affect the riser and drill pipe as shown in Fig. 11 and 12. The same conclusion was arrived when the drill pipe penetrates the surface at 50 m. Without any VIV interference, the drill string will return to its original position at the riser's vertical axis with a small displacement recorded.

Figure 13 shows a similar shifting pattern away from the riser's axis. Higher rotation speed at 300 RPM induced the increase of drill string frequency, with a different amplitude shape and pitches recorded compared with the 80 RPM. The maximum displacement of the drill string decreases significantly and shows that at 300 RPM speed, the drill string might already pass the critical speed.

Figure 14 shows the displacement plot at 5 Hz with 300 RPM speed. As the frequency increase the displacement of drill string decrease more compared with 0.5 Hz and shows that the drill string can withstand the effect of the vortex shedding forces.

Figure 15 shows the harmonic motion recorded at the bottom node of the drill strings throughout the working frequencies. The spike indicates the rising of the lateral displacement to the maximum level at 42 Hz. When a higher speed at 300 RPM applied to the system, the harmonic motion recorded with smaller spike and lower frequency at 30 Hz compared with low RPM.

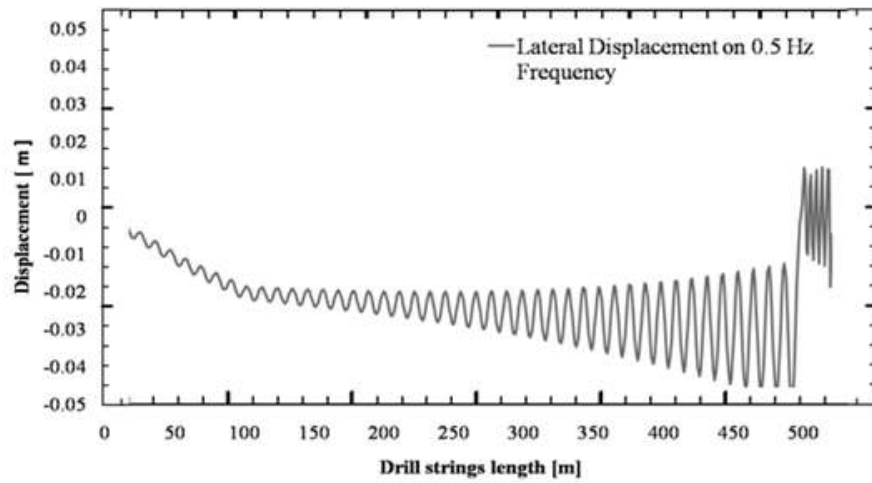


Fig. 11: Lateral displacement on 0.5 Hz at 80 RPM with vortex shedding forces

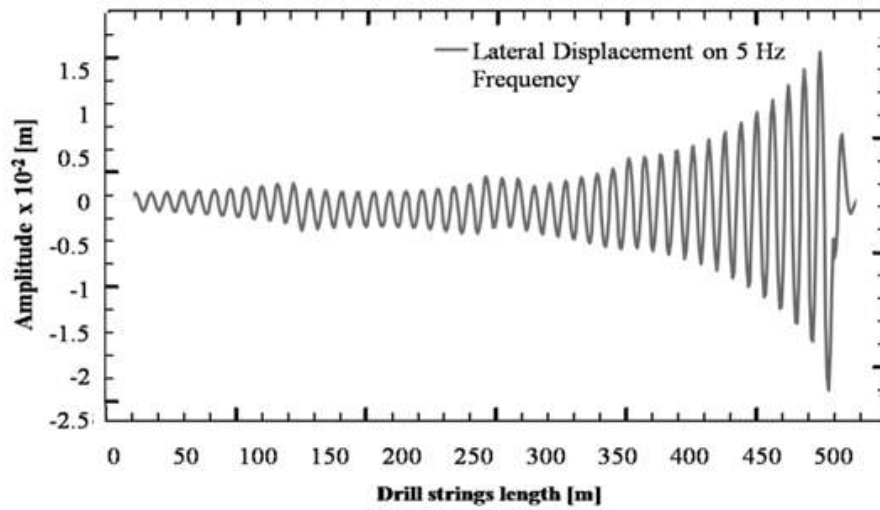


Fig. 12: Lateral displacement on 5 Hz at 80 RPM with vortex shedding forces

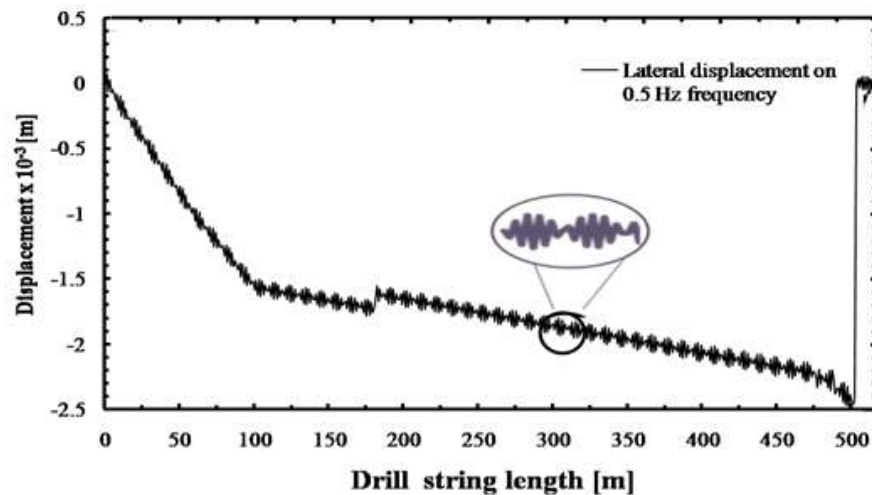


Fig. 13: Lateral displacement on 0.5 Hz at 300 RPM with vortex shedding forces

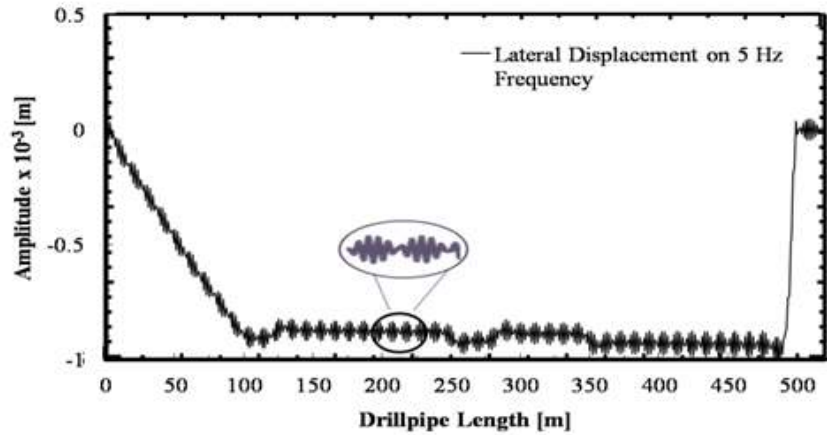


Fig. 14: Lateral displacement on 5 Hz at 300 RPM

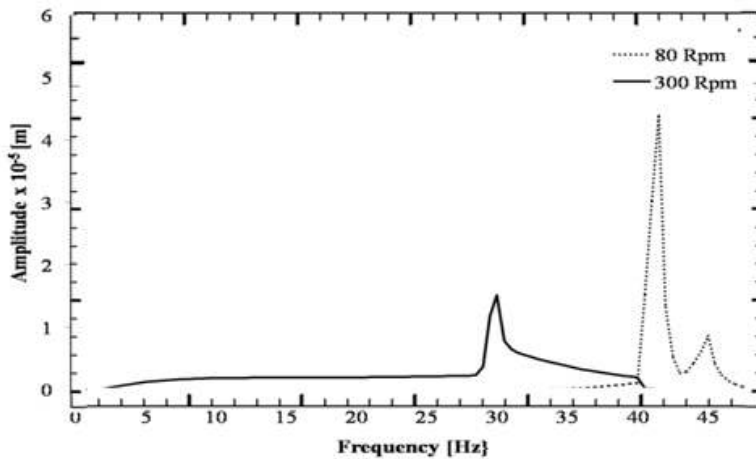


Fig. 15: Amplitude plot

The effect of vortex shedding vibration is apparent when the system drill pipe rotates at low RPM. The drill strings will displace more due to the frequency of drill strings is low and susceptible to external frequency interference. When the drill string rotates at higher speed, with an associated higher natural frequency than the vortex shedding resonance frequency, the maximum displacement at the bottom of drill string will decrease.

CONCLUSION

A finite element dynamic model of rotating drill string coupled to vortex shedding forces was developed using ANSYS. The model mimics the drilling operation in deep water when the riser is used to protect the drill strings inside. The hydrodynamic pressure and current speed increase the magnitude of the vortex shedding forces to the riser. The lateral vibration mode was analyzed at two conditions, with and without vortex shedding forces. The vortex forces contribute a significant effect to increase the vibration risk by deforming the drill string from its longitudinal axis. The

maximum effect of vortex shedding forces occurs at low frequency and small RPM. Rotational speed of drill string also influenced the effect of vibration. With a higher rotational speed at 300 RPM, it is concluded that drill string have already withstood the lateral vibration compared with low RPM at 80 RPM, confirmed with a small displacement occur in the drill string.

ACKNOWLEDGMENT

The first author will like to acknowledge the financial assistant by Universiti Teknologi PETRONAS under the Graduate Assistance Scheme. This research is funded by UTP Research and Innovation Grant URIF 31/2012.

REFERENCES

Aarsnes Flø, J.U., 2012. Reduced order observer design for managed pressure drilling. Department of Engineering Cybernetics, Norwegian University of Science and Technology.

- Aldushaishi, M.F., 2012. Investigation of drillstring vibration reduction tools. M.A. Thesis, Petroleum Engineering, Missouri University of Science and Technology.
- Bahr Khalil, M.K., 2009. Interactive analysis of closed loop electro-hydraulic control systems. Proceeding of the 13th International Conference on Aerospace Sciences and Aviation Technology. Cairo, Egypt, pp: 1-10.
- Bailey, J. and I. Finnie, 1960. An analytical study of drill string vibration. *J. Eng. Ind.*, 2(82): 122-128.
- Burgess, T.M., G.L. McDaniel and P.K. Das, 1987. Improving BHA tool reliability with drillstring vibration models: Field experience and limitations. Proceeding of the SPE/IADC Drilling Conference. New Orleans, Louisiana.
- Chen, S.S., M.W. Wambsganss and J.A. Jendrzejczyk, 1976. Added mass and damping of a vibrating rod in confined viscous fluids. *J. Appl. Mech.*, 43(September 1974): 325.
- Dixon, M. and D. Charlesworth, 2006. Application of CFD for vortex-induced vibration analysis of marine risers in projects. Proceeding of Annual Offshore Technology Conference. Houston, Texas.
- Ehsan, I., S. Mohammad, N.M. Reza and J. Ali, 2012. Laminar and turbulent power law fluid flow passing a square cylinder. *Int. J. Phys. Sci.*, 7(7): 988-1000.
- Gulyayev, V.I. and O.I. Borshch, 2011. Free vibrations of drill strings in hyper deep vertical bore-wells. *J. Petrol. Sci. Eng.*, 78(3-4): 759-764.
- Lien, F.S., P.A. Durbin and S. Parniex, 1997. Non-linear v²- f modeling with application to aerodynamic flows. Proceeding of the 11th Symposium on Turbulent Shear Flows. Grenoble, France, pp: 8-10.
- Lubcke, H., St. Schmidt, T. Rung and F. Thiele, 2001. Comparison of LES and RANS in bluff-body flows. *J. Wind. Eng. Ind. Aerod.*, 89(14-15): 1471-1485.
- Norwegian Oil Industry Association, 2010. Recommended Guidelines for Deployment of RFID ON-Drill String Components. 14th Edn., the Norwegian Oil Industry Association, Oslo.
- Sengupta, S., 1978. the effect of vortex shedding on marine risers. *SPE J.*, Document ID: 7667-MS.
- Sohankar, A., 2006. Flow over a bluff body from moderate to high reynolds numbers using large eddy simulation. *Comput. Fluids*, 35(10): 1154-1168.
- Whitney, A.K., L. Palo and K.G. Nikkel, 1983. Effects of shear flow on vortex-shedding-induced vibration of marine risers. Proceeding of the 15th Annual Offshore Technology Conference. Houston, Texas.
- Zare, J., S.J. Hashemi and G. Rashed, 2011. Finite element analysis of drillstring lateral vibration. *Sci. Res. Essays*, 6(13): 2682-2694.